
IMPACT OF NETWORK ASSORTATIVITY ON EPIDEMIC AND VACCINATION BEHAVIOUR

A PREPRINT

Sheryl L. Chang^{a *}
sheryl.chang@sydney.edu.au

Mahendra Piraveenan^{a,b}
mahendrarajah.piraveenan@sydney.edu.au

Mikhail Prokopenko^{a,c}
mikhail.prokopenko@sydney.edu.au

^aComplex Systems Research Group, Faculty of Engineering and IT
The University of Sydney, NSW, 2006, Australia

^bCharles Perkins Centre, The University of Sydney
John Hopkins Drive, Camperdown, NSW, 2006, Australia

^cMarie Bashir Institute for Infectious Diseases and Biosecurity
The University of Sydney, Westmead, NSW, 2145, Australia

September 12, 2022

ABSTRACT

The resurgence of measles is largely attributed to the decline in vaccine adoption and the increase in travels. Although the vaccine for measles is readily available and highly successful, its current adoption is not adequate to prevent epidemic. Vaccine adoption is directly affected by vaccination decisions from human behaviour and has a complex interplay with the spatial spread of disease specific to one's travelling network. In this paper, we focus on modelling the travelling network as scale-free network to investigate the correlation between the network's assortativity and the resultant epidemic and vaccination dynamics, by adopting a SIR-network model in game-theoretic framework with imitation dynamics under voluntary vaccination scheme. Our results show a non-linear correlation between epidemic dynamics and network's assortativity, highlighting that highly disassortative networks are particularly impactful at containing epidemics. To explain the finding, we propose a novel network-theoretic measure, ψ , defined as the ratio between Shannon information and maximum coreness. Higher ψ is found in highly disassortative networks, which provides an explanation on why disassortative networks may be better at suppressing epidemics. Furthermore, We find that ψ has a monotonically decreasing relationship with cumulative incidence, indicating that higher ψ corresponds to lower cumulative incidence.

Keywords Assortativity · Vaccination · Epidemic modelling · SIR model · Scale-free Networks

1 Introduction

The World Health Organization (WHO) reported resurgence of measles across the globe in recent years [1]. For example, in Australia, New South Wales (NSW) Government issued 6 measles alerts in 2019 in which most infected cases were imported from overseas [2]. Health authorities confirmed that the rise of the highly infectious yet vaccine preventable disease is largely due to the decline in vaccination coverage and the increase in domestic and international travels.

*Corresponding author

The high infectivity of measles is reflected by the high basic reproduction number (R_0), a measure defined as the average number of secondary cases arising from an infectious case in an otherwise susceptible population [3]. The epidemic threshold (for example, $R_0 = 1$) is related to critical regimes and phase transitions which can be interpreted by statistical physics [4, 5]. Diseases with $R_0 > 1$ typically develop into an epidemic with a rapid onset characterised by an exponential increase in prevalence [6]. The typical range of R_0 for measles is between 12 and 18, meaning that on average, each infectious individual with measles would infect 12 to 18 susceptible people [7].

For such a highly infectious disease like measles, high vaccine adoption is extremely important for epidemic containment. Vaccine adoption, driven by vaccination decisions from human behaviour, has been found very sensitive to many factors (e.g., cost of vaccination, disease prevalence, other individual's behaviours, etc.) and produces highly non-linear dynamics with oscillatory dynamics [8, 9]. Various complex human interactions attribute to travel and population mixing patterns, and so play a significant role in vaccine adoption. These non-trivial interactions are found to be particularly pronounced in scale-free networks [10].

This study combines several fundamental methodologies, drawing from game theory, network theory and information theory. Such a multi-disciplinary setting is required to address the key underlying challenges in computational epidemiology: time-dependent risks and varying imitation dynamics involved in vaccination decision-making, complex interaction and transmission patterns within the affected population, and nonlinear dependencies between the underlying network structure and the epidemic dynamics.

(i) Imitation dynamics: game-theoretic modelling Human behaviour with respect to vaccine adoption can be seen as a decision making process by individuals, as one would evaluate the benefits and weakness of a strategy (i.e., to vaccinate or not to vaccinate) and form a well-informed decision after trade-offs. This process is often modelled by game theory where rational and self-centred individuals reach a decision after comparing their payoffs of "to vaccinate" versus "not to vaccinate". Several previous studies found that vaccination behaviour exhibits oscillatory dynamics if individuals decide whether to vaccinate based on current disease prevalence and social learning (i.e., imitating other people's behaviour) if they are sufficiently responsive towards prevalence change [8, 9, 11].

(ii) Interaction patterns: network-theoretic methods A different challenge is that the spatial spread of infectious disease is dependent on topological connectivity within a population, with interactions only permitted between connected individuals [12]. This feature is addressed by using network-theoretic methods where interactions are only allowed between connected nodes, along the edges [12–16]. A network-theoretic component has been later introduced to model spatial spreading through two approaches:

- (a) Local: person-to-person contacts at individual level where each individual is modelled as a node and infection is only possible along edges [17–24], and
- (b) Global: meta-population level where each node represents a residential locality and people move across connected nodes [25–27].

Integrated with networks, recent models extend the game-theoretic framework to include imitation dynamics where the imitation process is defined by network topology. The imitation process can take place at a local level by imitating one's neighbours. [18–23], or at a global level by imitating the most successful strategy at one's residential locality resulting from travelling and population mixing [27].

The topology of an underlying network plays a crucial role in the spreading process [10, 28]. Diverse topological impacts could be quantified by a multiplicity of network measures. In particular, assortativity has been shown to correlate with the duration of an epidemic [29], the maximum eigenvalue of the adjacency matrix correlates with the epidemic threshold [30, 31], and the maximum coreness identifies key spreaders in a network [32].

(iii) Nonlinear effects: information-theoretic approaches The epidemic spread is constrained by the underlying contact network, and at the same time, the interaction patterns change in response to epidemics. This dependency is not dissimilar to the well-known structure-function duality observed in complex networks, where the function is constrained by the structure and the structure evolves due to function [33, 34]. To account for non-linear dependencies between structure and dynamics, information theory has been applied to quantify the complexity of an information dynamics within networks [35–38]. For example, Shannon information content of a network has been used to characterise the contribution of topological constraints to both entropy and assortative noise in complex networks [39]. This was followed by Piraveenan et al., 2012 [40] in information-theoretically quantifying the assortative mixing in directed networks. This approach identified the "regulator" nodes which are dominant in network connectivity, driving the "regulatee" nodes. Other information theoretic measures, such as active information storage and transfer entropy, have been used to capture the critical transitions in epidemic dynamics [5].

Furthermore, highly connected nodes (i.e., hubs), commonly observed in empirical networks and scale-free networks, are particularly critical to containing epidemics [10, 18]. However, not all hubs have equal impacts in the spreading process. For example, hubs located at the core (i.e., having maximum coreness) in assortative network have greater impact in the spreading process because they sustain an epidemic in a small, dense segment [29, 32].

In this paper, we focus on the role of assortativity in scale-free networks with the vaccine adoption resulting from human behaviour, adopting a game-theoretic framework with imitation dynamics. Our main contribution lies in untangling the interplay between the travelling pattern and the global vaccination and epidemic dynamics, in order to gain a better understanding of the non-linear dynamics which characterises both epidemics and vaccination behaviour. By setting up the travelling pattern as a scale-free network, we specifically investigate the role of the network’s assortativity in the resultant epidemic and vaccination dynamics. We are able to produce complex oscillatory dynamics for a range of assortativity (and disassortativity) values. The results are also evaluated with respect to the maximum eigenvalue of the adjacency matrix, in order to analyse the dynamics in relation to network robustness and stability of the dynamics. In doing so, we uncover the non-linear correlation between epidemic dynamics and assortativity in scale-free networks and highlight the important role of disassortative networks in containing epidemics. Our secondary contribution is to explain this dependency by proposing a new network-theoretic measure, ψ , defined as the ratio between the network’s Shannon information content and its maximum coreness. The proposed measure shows that the higher ψ observed in disassortative networks corresponds to lower cumulative incidence in scale-free networks, and therefore explains why highly disassortative networks are particularly impactful at containing epidemic.

The rest of this paper is structured as follows. Section 2 describes the model (Section 2.1) and network configurations (Section 2.2). Section 3 shows the simulation results obtained in a series of scale-free networks. Finally, Section 4 summarizes the findings.

2 Materials and methods

2.1 Model

We adopt a model that considers the vaccination game with imitation dynamics where the population’s vaccination decision depends on the current prevalence and vaccine adoption at their travelling destination [27].

Consider a network with M nodes, in which each node represents a suburb, $i \in V$, where $i = 1, 2, \dots, M$ [25, 26]. Travelling is only allowed between directly linked nodes i and j without hops on a daily basis where a fraction of population living in node i can travel to node j and back, and vice-versa. The connectivity of suburbs and the fraction of people commuting between them are represented by the population flux matrix ϕ . Entries in ϕ represent the fraction of population daily commuting from i to j , $\phi_{ij} \in [0, 1]$ (Equation 1). Some individuals may stay at their residential node (i.e. diagonal matrix $\text{diag}(\phi_{11}, \phi_{22}, \dots, \phi_{MM}) \neq 0$) and population of each node is conserved so that each row in ϕ sums to 1.

$$\phi_{M \times M} = \begin{bmatrix} \phi_{11} & \phi_{12} & \cdots & \phi_{1M} \\ \phi_{21} & \phi_{22} & \cdots & \phi_{2M} \\ \vdots & \vdots & \ddots & \vdots \\ \phi_{M1} & \phi_{M2} & \cdots & \phi_{MM} \end{bmatrix} \quad (1)$$

To reach a vaccination (or non-vaccination) decision, unvaccinated susceptible individuals’ decision-making process depends on two factors: the risk of infection based on current prevalence, and the most successful strategy based on social learning behaviour. At each time step, unvaccinated individuals evaluate their payoffs by weighing on the risk of vaccination from morbidity (f_v) and risk of non-vaccination from infection (f_{nv}), shown as:

$$\begin{aligned} f_v &= -r_v \\ f_{nv} &= -r_{nv}mI(t) \end{aligned} \quad (2)$$

where r_v is the morbidity from vaccination, r_{nv} is the morbidity from infection, m is individuals’ sensitivity to prevalence, and $I(t)$ is the current disease prevalence in population fraction at time t .

To make one switch to a vaccinating strategy, the payoff gain must be positive $f_v - f_{nv} > 0$. Individuals may also switch to a vaccinating strategy by imitating others (i.e., ‘imitation dynamics’), provided vaccination is the most successful strategy in the population.

Let x denote the relative proportion of vaccinated individuals, and assume that individuals use the combined imitation rate δ to sample and imitate strategies of other individuals. Then the time evolution of x can be defined as:

$$\begin{aligned}\dot{x} &= \delta(1-x)x[-r_v + r_{nv}mI] \\ &= \kappa x(1-x)(-1 + \omega I)\end{aligned}\quad (3)$$

where $\kappa = \delta r_v$ and $\omega = mr_{nv}/r_v$ [8].

Vaccination is an irreversible process, meaning that a vaccinated individual cannot revert back to the unvaccinated status. Therefore, only a non-vaccinated individual could imitate a vaccinated individual's strategy. It is also assumed that vaccination is only provided to susceptible newborns with life-long protection against measles, meaning that individuals will not need to re-vaccinate.

Since both imitation and the current disease prevalence are based on the individual's travelling pattern, Equation 3 is extended in a network setting. For any node $i \in V$, let x_i denote the fraction of vaccinated individuals in suburb i . Each day, unvaccinated susceptible individuals $(1 - x_i)$ travel to suburb j and encounter vaccinated individuals from node k . Every time a non-vaccinated person from i comes in contact with a vaccinated person from k , the imitation of the 'vaccinate' strategy takes place with a combined imitation rate (δ) to the difference in payoffs, $f_v - f_{nv}$. The rate of change of the proportion of vaccinated individuals in i over time (i.e., the daily increase in x_i) can then be expressed by:

$$\begin{aligned}\dot{x}_i &= \delta(1-x_i) \sum_{j=1}^M \sum_{k=1}^M \phi_{ij}(-r_v + r_{nv}mI_j)\phi_{kj}x_k \\ &= \kappa(1-x_i) \sum_{j=1}^M \sum_{k=1}^M \phi_{ij}(-1 + \omega I_j)\phi_{kj}x_k\end{aligned}\quad (4)$$

The vaccination dynamics is then coupled with a standard SIR model where the population at each node is categorised as susceptible (S), infected (I), and recovered (R). Successfully vaccinated newborns are directly transferred to the recovered class. Within each suburb (i.e., node), population is homogeneous and conserved over time. In essence, the model divides the population into many homogeneous groups [3], based on their residential suburbs. The model is given by:

$$\begin{aligned}\dot{S}_i &= \mu(1-x_i) - \sum_{j=1}^M \sum_{k=1}^M \beta_j \phi_{ij} \frac{\phi_{kj} I_k}{\epsilon_j^p} S_i - \mu S_i \\ \dot{I}_i &= \sum_{j=1}^M \sum_{k=1}^M \beta_j \phi_{ij} \frac{\phi_{kj} I_k}{\epsilon_j^p} S_i - \gamma I_i - \mu I_i \\ \dot{R}_i &= \mu x_i + \gamma I_i - \mu R_i \\ \dot{x}_i &= \kappa(1-x_i) \sum_{j=1}^M \phi_{ij}(-1 + \omega I_j) \sum_{k=1}^M \phi_{kj} x_k\end{aligned}\quad (5)$$

where ϵ_j^p is a normalisation factor as the ratio between present population N_j^p and the residential population N_j , and $\epsilon_j^p = \frac{N_j^p}{N_j} = \frac{\sum_{i=1}^M \phi_{ij} N_i}{N_j}$.

The dynamics of epidemic and vaccination at each node is computed individually and the global epidemic dynamics of the entire network can be obtained by summing over all nodes.

2.2 Network properties and Shannon information

Scale-free networks follow a power-law degree distribution with a few highly connected nodes (i.e., hubs) and numerous small-degree nodes. Such a tendency is commonly observed in real-world networks (e.g., air-traffic network, actor network, and the World Wide Web (WWW), etc.). Formally, the power-law distribution is defined as [41]:

$$P(k) = Ak^{-\gamma}u(k/N_p)\quad (6)$$

where u is a step function specifying a cut-off at $k = N_p$.

Assortative mixing, measured by assortativity coefficient, r ($-1 \leq r \leq 1$), is a preference for network nodes to connect to similar nodes where similarity can be defined in many ways, for example, in terms of node degree [29, 41]. For example, if highly connected nodes tend to connect to each other (e.g., actor network), the network is assortative ($r > 0$); if highly connected nodes tend to link to small-degree nodes instead (e.g., the protein-interaction network of yeast), the network is disassortative ($r < 0$). Our focus is to investigate the correlation between the assortativity and the epidemic severity. To do so, we will vary the assortativity of a scale-free network while preserving its scale-free properties. Xalvi-Brunet and Sokolov algorithm is used to rewire a scale-free network to a desired level of assortativity [42] (see Appendix A for more details on rewiring algorithm).

A k -core is a maximal sub-network such that its nodes have at least k degrees [43, 44]. k -core is obtained by recursively deleting all nodes of degrees less than k and their edges and the remaining network is the k -core. This process is called k -shell decomposition [45]. We are interested in the maximum k -core (i.e., maximum coreness), k_s , which characterises the nodes located in the innermost shell. In assortative networks, many of these nodes located at the core of the network are hubs and have been shown to be "influential spreaders" for forming a reservoir to sustain epidemic spreading [29, 32], prolonging the duration of an epidemic outbreak. In disassortative networks, however, hubs are located at the periphery of the network and tend to be connected to peripheral nodes, suppressing epidemic spread and resulting in shorter epidemic periods [32].

The maximum eigenvalue of the adjacency matrix, λ_{max} , has been related to the network's robustness during diffusion processes (e.g., virus propagation) [46]. Importantly, λ_{max} is in an inverse relationship with the epidemic threshold (τ) for arbitrary graphs ($\tau = 1/\lambda_{max}$), indicating that networks with higher λ_{max} will have lower epidemic threshold. These networks, therefore, are more vulnerable in disease propagation by node infection [30, 31].

The amount of information contained within a network has been quantified by Shannon information [38, 47]:

$$I(q) = \sum_{j=0}^{N_p-1} \sum_{k=0}^{N_p-1} e_{j,k} \log \frac{e_{j,k}}{q_j q_k} \quad (7)$$

where $e_{j,k}$ is the joint probability distribution of the remaining degrees of the two nodes at either end of a randomly chosen edge, and q_k is the remaining degree which is defined in relation to the degree distribution p_k as:

$$q_k = \frac{(k+1)p_{k+1}}{\sum_j^{N_p} j p_j}, \quad 0 \leq k \leq N_p - 1 \quad (8)$$

where k is the degree of a randomly chosen node ($1 \leq k \leq N_p$).

Previous studies [29, 48, 49] found that assortativity r is closely related to the information content $I(q)$, the maximum coreness k_s , and the maximum eigenvalue λ_{max} . As r increases, both λ_{max} and k_s increase monotonically in the entire assortative (and disassortative) range ($-1 \leq r \leq 1$) [29, 49]. Shannon information content of scale-free networks, however, increases non-linearly and asymmetrically with the absolute value of assortativity [48]. We illustrate these dependencies in Figure 1.

In addition to the existing measures, we propose a new measure, ψ , as the ratio between Shannon information and maximum coreness, defined as:

$$\psi = \frac{I(q)}{k_s} \quad (9)$$

We find that ψ increases non-linearly and asymmetrically with the absolute value of r in a way that high disassortativity corresponds to the highest ψ (Figure 1 (b)). In other words, a highly disassortative network has greater information content per maximum coreness than its assortative counterpart, whereas non-assortative networks always have the lowest information content per maximum coreness. This observation suggests that both highly disassortative networks and highly assortative networks may be less vulnerable to epidemic than non-assortative networks. In particular, highly disassortative networks may be better at containing epidemics. We verify these conjectures by simulating epidemic spread across a range of scale-free networks, varying their assortativity while preserving the degree distribution.

Without loss of generality, we set the epidemiological parameters to a scenario motivated by measles epidemic ($R_0 = 15$ [7]) while assuming uniform initial conditions and population's responsiveness towards prevalence change across all nodes. A small fraction of initial infected population is deployed in all nodes to evaluate the impact of travelling diffusion. Refer to Table 2 in Appendix B for all parameters used.

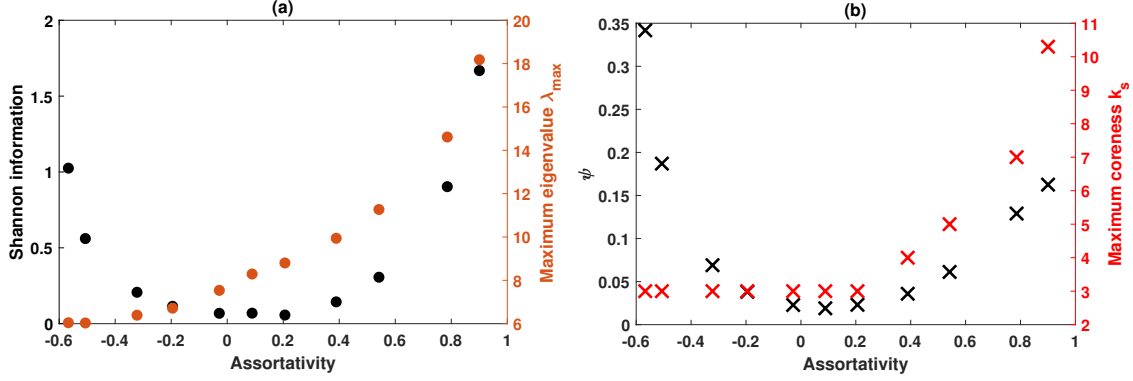


Figure 1: Scale-free networks: relationships between assortativity and other network measures. (a) Shannon information (left y-axis, in black), maximum eigenvalue (right y-axis, in red), λ_{max} , and (b) Information coreness ratio, ψ (left y-axis, in black), maximum coreness, k_s (right y-axis, in red). Network properties: $\gamma = 2.75$, $\langle k \rangle \approx 4$, $k_0 = 1$. Each data point is averaged over 10 runs.

3 Simulation results

We first analyse how assortativity affects the severity of epidemics and vaccination dynamics, and then explain the results using the proposed measure, ψ . The severity of epidemics is quantified by the prevalence peak (I) and the cumulative incidence (i.e., proportion of newly infected individuals in the population at risk) during the first outbreak where the maximum prevalence occurs. See Appendix B for more details about the relationship between disease prevalence and cumulative incidence.

(i) **Oscillatory dynamics.** Figure 2 and Figure 3 show the oscillatory dynamics in disease prevalence (I) and vaccine adoption (x) for the networks across the simulated assortativity range ($-0.5671 \leq r \leq 0.9002$). The oscillations indicate that responsive individuals would react to changes in prevalence and consequently choose to vaccinate, however, high level of vaccine adoption is unable to sustain as soon as prevalence drops [8, 27]. As a result, individuals would consequently choose the non-vaccination strategy because the risk of infection is low since there is no change in disease prevalence. Moreover, we find that prevalence and vaccine adoption both reach early convergence to the mixed, endemic equilibrium in highly assortative (i.e., $r \approx 0.8976$) and highly disassortative networks (i.e., $r \approx -0.5736$). In addition, the first outbreak in highly disassortative networks occurs noticeably earlier at lower prevalence peak ($I_{max} \approx 0.0035$). The early convergence and premature peaks correspond to lower level of vaccine adoption, which concurs with the established results that high vaccine adoption under voluntary vaccination scheme is unattainable when disease prevalence is low [8, 9, 11, 50].

To account for network variability, each rewiring setting is then repeated for 10 scale-free networks of the same scale-free properties. For better readability, only prominent peaks in x and I are shown in Figure 4 and 5. In agreement with the results shown in Figure 2 and Figure 3, we observe a clear correlation profile between prevalence peak and the network's assortativity (or disassortativity), which shows that epidemics are generally better contained in highly assortative and highly disassortative networks.

(ii) **Correlation between network measures and epidemic severity.** To further evaluate the severity of the epidemic, we investigate the relationship between assortativity and the cumulative incidence under different initial vaccine adoption.

Figure 6 and Figure 7 show that topological impacts become significantly more pronounced when the initial vaccine adoption (x_0) is sufficiently high (i.e., $x_0 = 0.95$), while the influence of topology is negligible when initial vaccine adoption is low. These effects are traced in terms of both the maximum prevalence (Figure 6) and cumulative incidence (Figure 7). In particular, focusing on the case with high initial vaccine adoption (i.e., herd immunity), shown in Figure 6.(f) and Figure 7.(f), we observe that cumulative incidence is lower in disassortative networks (i.e., $r \approx -0.5671$) and assortative networks (i.e., $r \approx 0.9002$). In contrast, the population is at the highest risk (i.e., having the highest cumulative incidence) in non-assortative networks (i.e., $r \approx 0.0889$).

Similar dependency is also observed in terms of the maximum eigenvalue of the adjacency matrix, λ_{max} (Figure 8). We find that both r and λ_{max} display a non-monotonic profile with cumulative incidence that is consistently the lowest in disassortative networks.

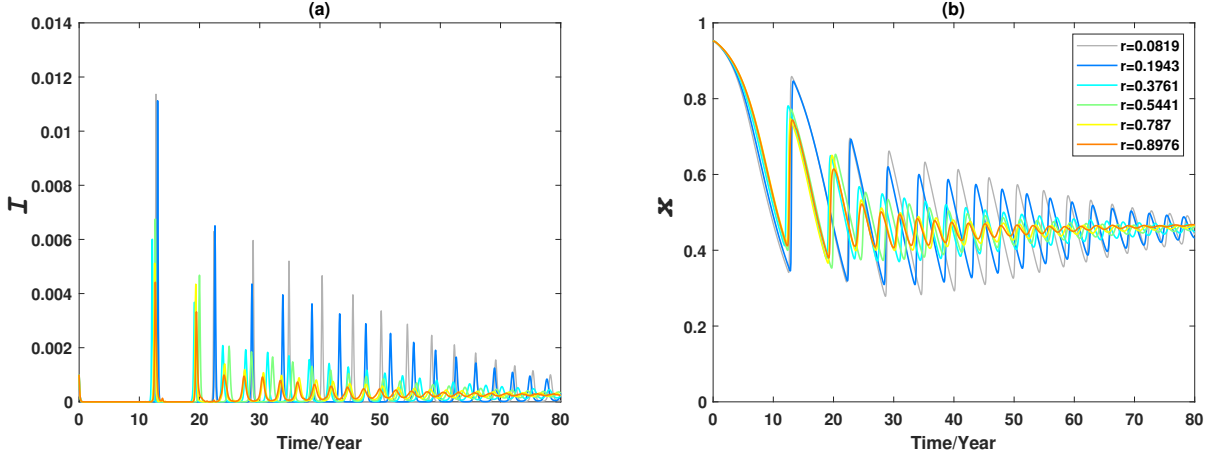


Figure 2: Epidemic dynamics of a set of scale-free networks ($N = 3000, \gamma = 2.75, k_0 = 1, \langle k \rangle \approx 4$), with assortative rewiring. Time series of (a) I , disease prevalence, and (b) x , frequency of vaccinated individuals. Initial conditions: $I_0 = 0.001, S_0 = 0.05, x_0 = 0.95$. Behaviour parameters: $\omega = 3500, \kappa = 0.001$

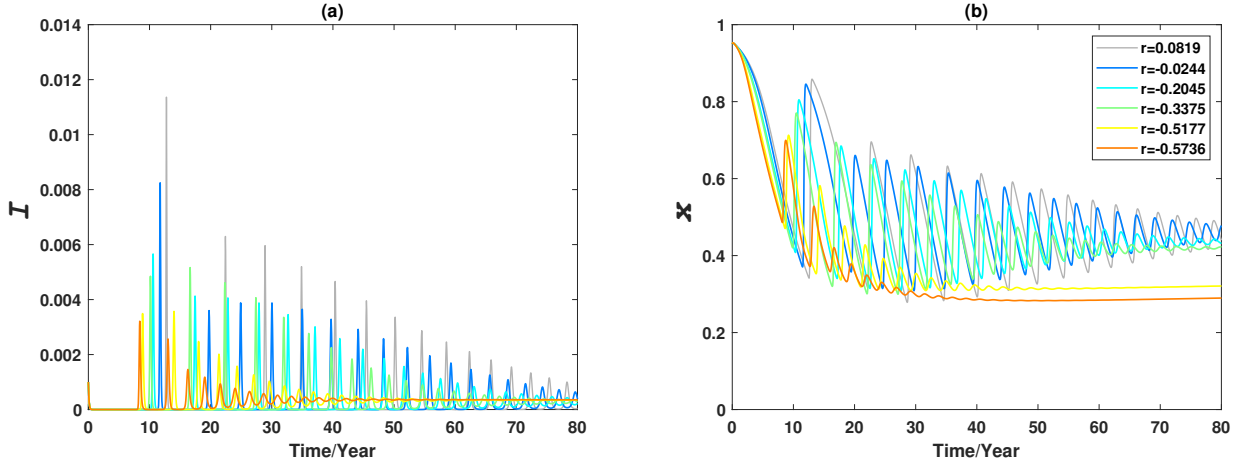


Figure 3: Epidemic dynamics of a set of scale-free networks ($N = 3000, \gamma = 2.75, k_0 = 1, \langle k \rangle \approx 4$), with disassortative rewiring. Time series of (a) I , disease prevalence, and (b) x , frequency of vaccinated individuals. Initial conditions: $I_0 = 0.001, S_0 = 0.05, x_0 = 0.95$. Behaviour parameters: $\omega = 3500, \kappa = 0.001$

Both these profiles, obtained for the case of herd immunity in terms of the assortativity coefficient (Figure 6.(f)) or the maximum eigenvalue (Figure 7.(f)), display a non-linear character, showing that these network measures cannot be used as simple predictors of epidemic severity. The proposed measure, ψ , on the contrary, displays a monotonically decreasing profile with cumulative incidence (Figure 9). Low ψ ($\psi < 0.03$) corresponds to non-assortative networks ($-0.0282 \leq r \leq 0.2060$) with high cumulative incidence ($CI \approx 0.06$). Mid-high range of ψ ($0.03 < \psi < 0.17$) corresponds to either mid-to-highly assortative networks ($0.3891 \leq r \leq 0.9002$), or moderately disassortative networks ($-0.332 \leq r \leq -0.1952$), all of which correspond to lower cumulative incidence ($CI \approx 0.05$). Finally, the higher ψ ($0.17 < \psi < 0.35$) corresponds to highly disassortative networks ($-0.5671 \leq r \leq -0.5065$) with the lowest cumulative incidence ($CI < 0.04$).

4 Conclusion

In this work, we investigated how assortativity affects epidemic and vaccination dynamics in scale-free networks by adopting a game-theoretical SIR-network model with imitation dynamics. We first illustrated the dependencies between assortativity and other network-theoretic measures (i.e., maximum coreness (k_s), maximum eigenvalue of adjacency matrix (λ_{max}) and Shannon information). While k_s and λ_{max} increase monotonically with assortativity for

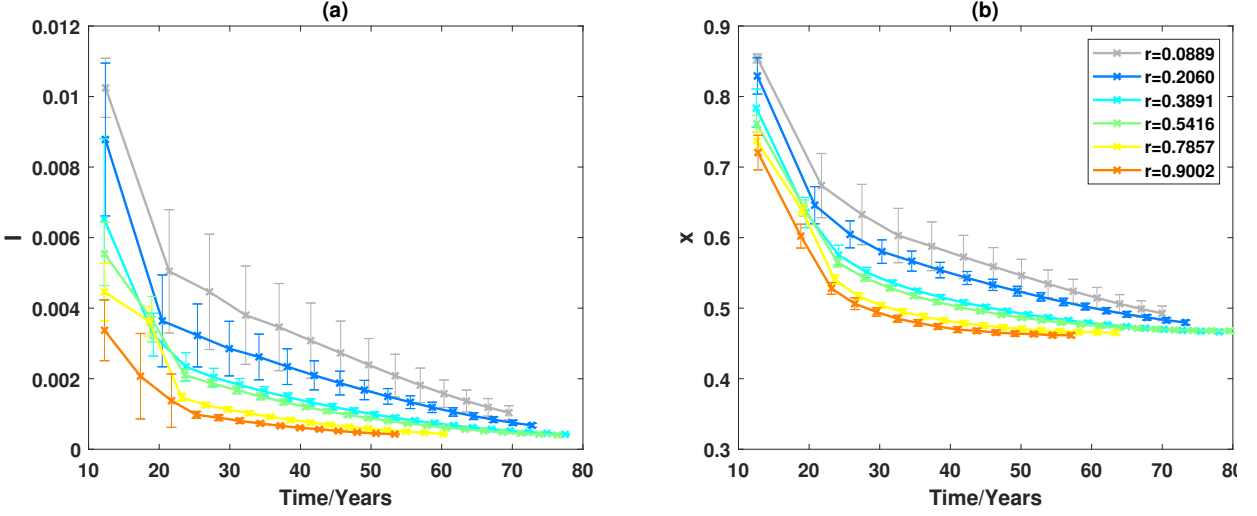


Figure 4: Epidemic dynamics of scale-free network ($N = 3000, \gamma = 2.75, k_0 = 1, \langle k \rangle \approx 4$), with assortative rewiring. Time series of peak amplitude for x , frequency of vaccinated individuals (a), and I , disease prevalence (b). Each data point is the average of 10 runs at the same setting. Error bars denote standard deviation. Peaks amplitudes are identified if the differences between adjacent peaks are greater than threshold value $\hat{x} = 0.01, \hat{I} = 0.0002$. Initial conditions: $I_0 = 0.001, S_0 = 0.05, x_0 = 0.95$. Behaviour parameters: $\omega = 3500, \kappa = 0.001$

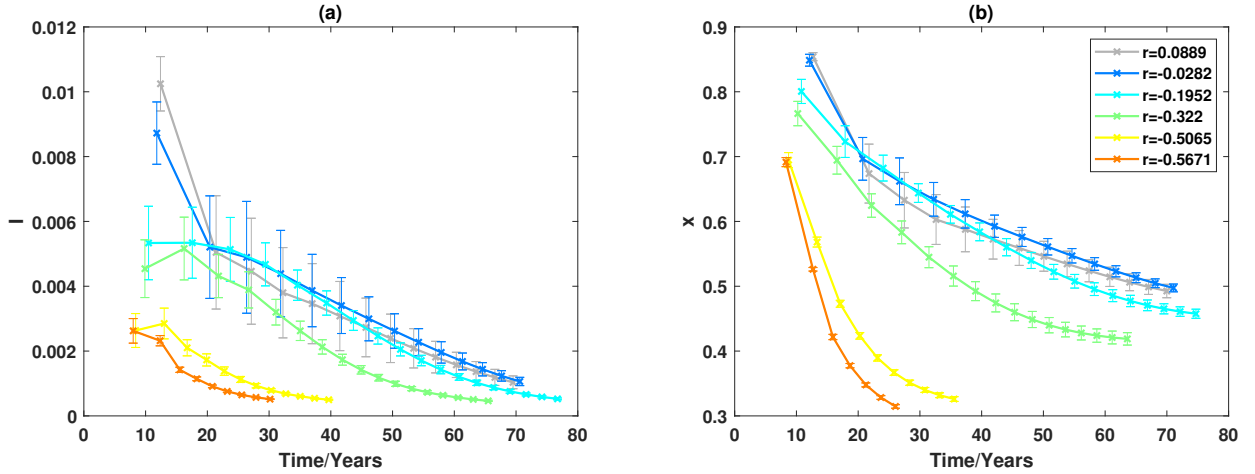


Figure 5: Epidemic dynamics of scale-free network ($N = 3000, \gamma = 2.75, k_0 = 1, \langle k \rangle \approx 4$), with disassortative rewiring. Time series of peak amplitude for x , frequency of vaccinated individuals (a), and I , disease prevalence (b). Each data point is the average of 10 runs at the same setting. Error bars denote standard deviation. Peaks amplitudes are identified if the differences between adjacent peaks are greater than threshold value $\hat{x} = 0.01, \hat{I} = 0.0002$. Initial conditions: $I_0 = 0.001, S_0 = 0.05, x_0 = 0.95$. Behaviour parameters: $\omega = 3500, \kappa = 0.001$

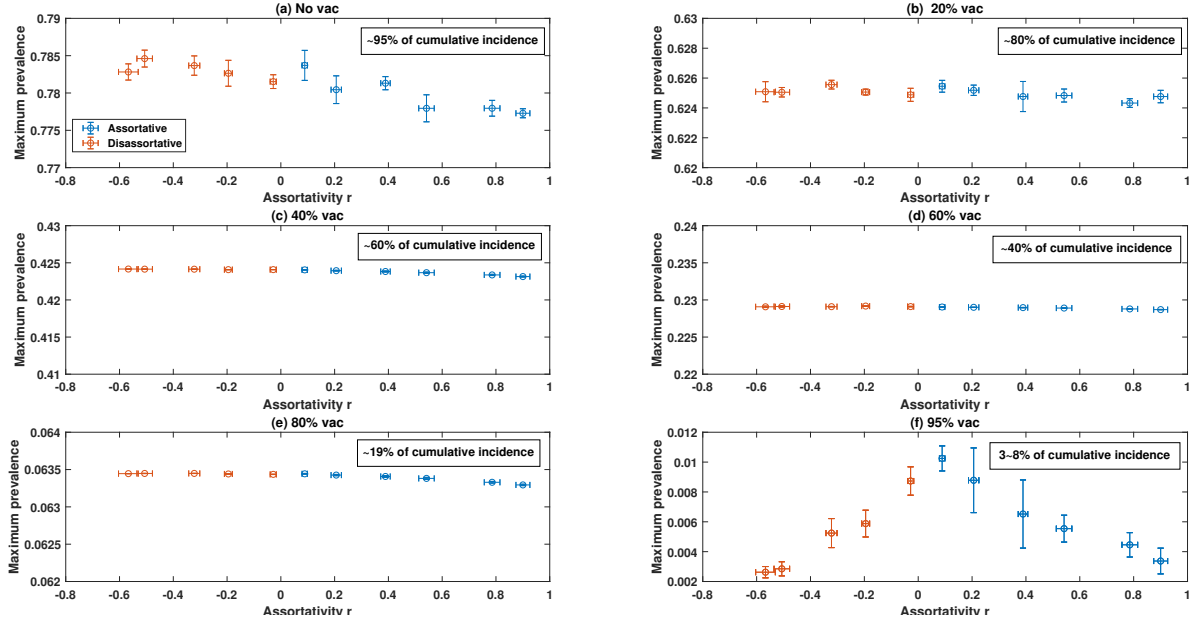


Figure 6: Maximum prevalence, I_{max} , in relation to assortativity, r . Data is extracted from Figure 1, Figure 4, and Figure 5. (a) - (f) correspond to different initial condition of vaccination. Error bars denote standard deviation over 10 runs.

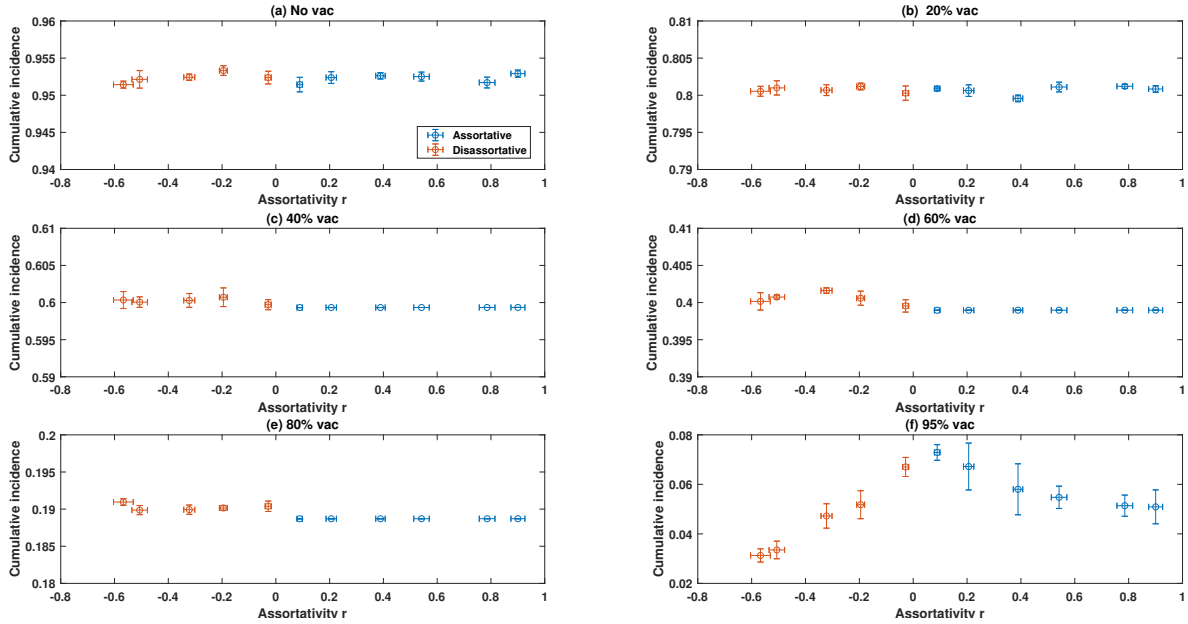


Figure 7: Cumulative incidence of the first outbreak in relation to assortativity, r . Data is extracted from Figure 1, Figure 4, and Figure 5. (a) - (f) correspond to different initial condition of vaccination. Error bars denote standard deviation over 10 runs.

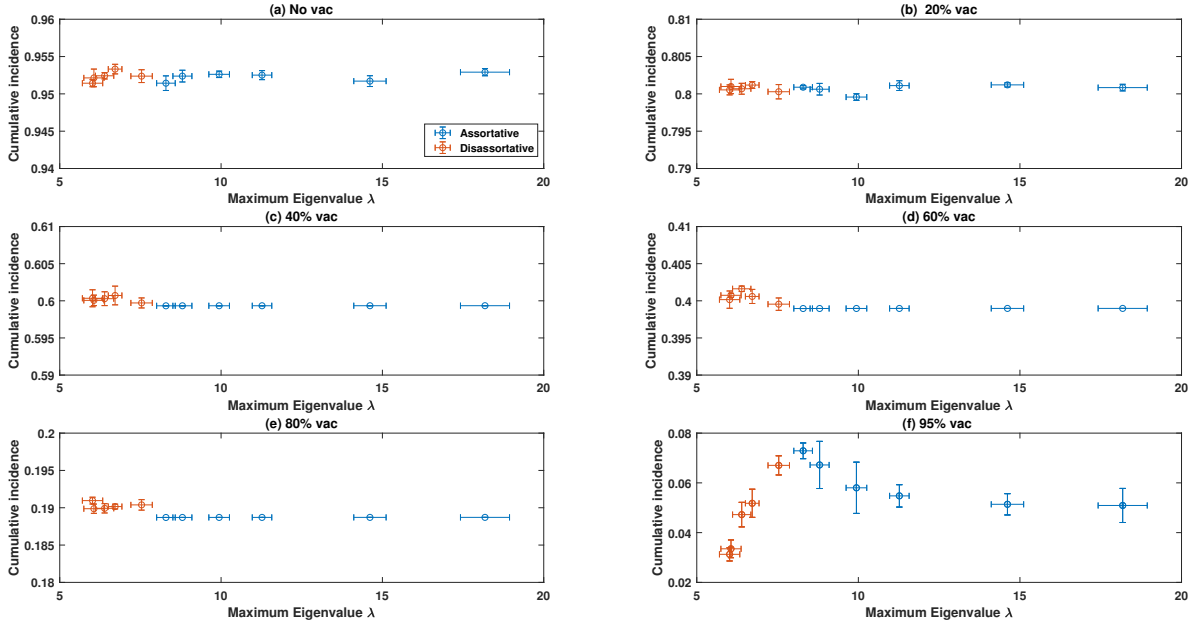


Figure 8: Cumulative incidence of the first outbreak in relation to maximum eigenvalue, λ_{max} . Data is extracted from Figure 1, Figure 4, and Figure 5. (a) - (f) correspond to different initial condition of vaccination. Error bars denote standard deviation over 10 runs.

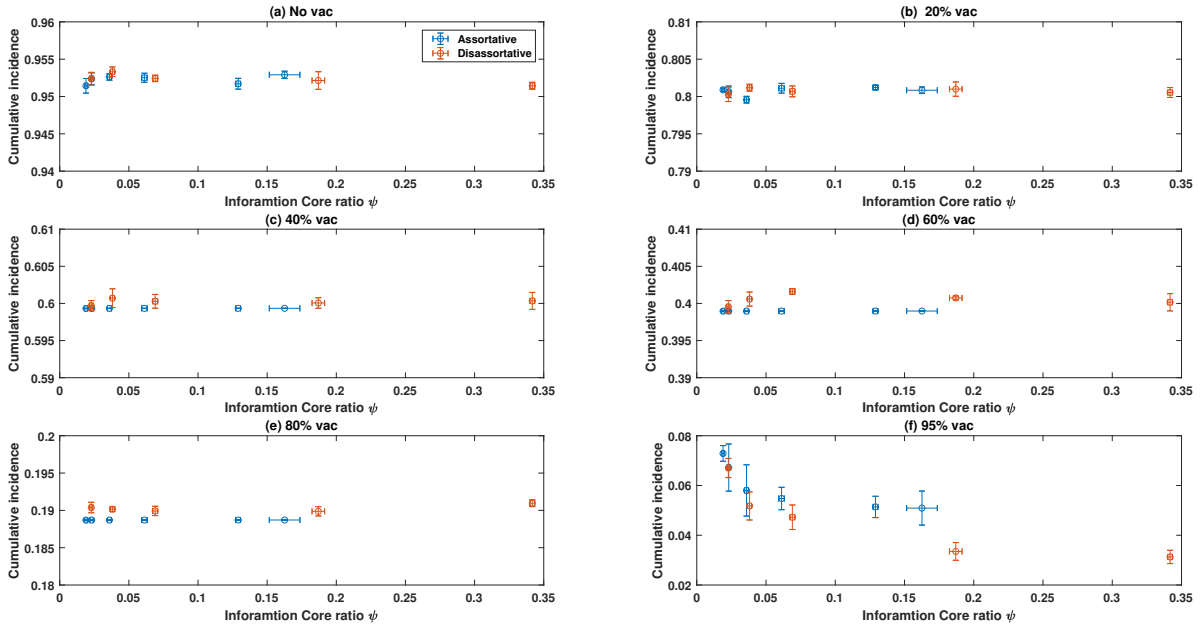


Figure 9: Cumulative incidence of the first outbreak in relation to Shannon information per maximum coreness, ψ . Data is extracted from Figure 1, Figure 4, and Figure 5. (a) - (f) correspond to different initial condition of vaccination. Error bars denote standard deviation over 10 runs.

the tested assortativity range ($-1 \leq r \leq 1$), Shannon information content of network increases with the absolute value of assortativity in a non-linear, asymmetric fashion.

We then proposed a new network-theoretic measure, ψ , as the ratio between Shannon information and maximum coreness. ψ was found to increase with the absolute value of assortativity and reached maximum in highly disassortative networks. Such a finding suggested that disassortative networks may be better at suppressing epidemics and this conjecture was verified by the simulations of epidemic spread on scale-free networks with varying assortativity.

In simulation results, oscillatory dynamics in both disease prevalence (I) and vaccine adoption (x) over time was observed, which concurs with Bauch, 2005 [8] and Bhattacharyya and Bauch, 2011 [50]. When I converges to the mixed, endemic equilibrium, the absence of change of prevalence also leads to converged equilibrium in vaccine adoption typically under 50%. To evaluate the severity of epidemics, we computed cumulative incidence during the first outbreak and found good agreement with the results from disease prevalence. Moreover, the existing network-theoretic measures (i.e., r and λ_{max}) displayed a non-mono-tonic correlation with the cumulative incidence. In non-assortative networks, cumulative incidence is at the highest, whereas in assortative and disassortative networks, cumulative incidence is at a lower level although r and λ_{max} in these networks are drastically different. The proposed measure ψ , on the other hand, displayed a monotonically decreasing correlation with the cumulative incidence so that disassortative networks with the highest ψ ($r \approx -0.5671, \psi \approx 0.34$) always correspond to the lowest cumulative incidence, a feature that is not captured by r or λ_{max} .

In summary, the proposed measure ψ provides an explanation on why disassortative scale-free networks are particularly impactful at containing epidemics compared to the assortative and non-assortative counterparts.

Declaration of interest

The authors declare no competing interests.

Acknowledgement

This research was funded by the Australian Research Council (ARC) Discovery Project grant DP160102742. Additionally, S. L. C was supported by an Australian Government Research Training Program (RTP) Scholarship. Furthermore, this research was supported by the Sydney Informatics Hub at the University of Sydney, through the use of High Performance Computing (HPC) services.

Appendices

Appendix A: Assortative rewiring

Assortativity here, r , is quantified by the Pearson correlation coefficient of the degrees at either ends of an edge ($-1 \leq r \leq 1$). For $r = 0$, the network is neutral; for $r < 0$, the network is disassortative; and for $r > 0$, the network is assortative [29, 41]. For scale-free networks, it has been found that the level of assortativity is constrained by the scale-free degree sequence of networks and bounded by the maximally disassortative and assortative mixing [51]. A higher scale-free exponent, γ , has a wider range of possible assortativity between r_{min} (maximally disassortative) and r_{max} (maximally assortative) within the scale-free regime ($2 \leq \gamma \leq 3$) [41]. We, therefore, choose $\gamma = 2.75$ as the scale-free exponent and use the Barabási-Albert model with random preferential attachment rate, $m \in [1, 3]$, to construct scale-free networks from a simple 3-node fully connected network while preserving terminal nodes using [52].

To achieve the desired level of assortativity, we use Xalvi-Brunet and Sokolov algorithm to rewire a scale-free network while preserving its power-law degree distribution and scale-free properties [42]. The rewiring algorithm is as follows:

1. Randomly select two links and locate four nodes of the selected edges.
2. Order the four nodes with respect to their degrees (k) from high to low (a, b, c, d where $k_a > k_b > k_c > k_d$).
3. For assortative rewiring, links are formed between nodes with similar degrees (i.e., $(a, b), (c, d)$). For disassortative rewiring, links are formed between nodes with polarising degrees (i.e., $(a, d), (b, c)$).
4. If the new links already exist in the network, the rewiring step is discarded. Go back to step 1 to select a new pair of links.

Steps	r_a	S_a	r_d	S_d
0	0.0889 [0.0783,0.1053]	0.0101	0.0889 [0.0783,0.1053]	0.0101
700	0.2060 [0.1844,0.2430]	0.0259	-0.0282 [-0.0459,-0.0120]	0.0366
2000	0.3891 [0.3695,0.4297]	0.0176	-0.1952 [-0.2218,-0.1711]	0.0147
3500	0.5416 [0.5098,0.6114]	0.0288	-0.3220 [-0.2997,-0.3716]	0.0205
8000	0.7857 [0.7568,0.8592]	0.0192	-0.5065 [-0.5813,-0.4782]	0.0115
15000	0.9002 [0.8733,0.9616]	0.0292	-0.5671 [-0.6571,-0.5281]	0.0289

Table 1: Assortative or disassortative rewiring using Xalvi-Brunet and Sokolov algorithm. Assortativity coefficient is averaged over 10 runs. r_a : assortivity; r_d : disassortivity; bracket shows the range of r_a and r_d for 10 runs. S_a : standard deviation of r_a ; S_d : Standard deviation of r_d .

Clearly, higher assortativity (and disassortivity) can be achieved by higher number of rewiring. We rewire a scale-free network to achieve 11 different levels of assortativity within $-1 \leq r \leq 1$. Table 1 summarises how r changes with changing number of assortative and disassortative rewiring. Figure 10 and 11 show the inner regularity of scale-free networks when nodes connect to other nodes with similar degree (Figure 10) and nodes that connect to nodes with different degrees (Figure 11).

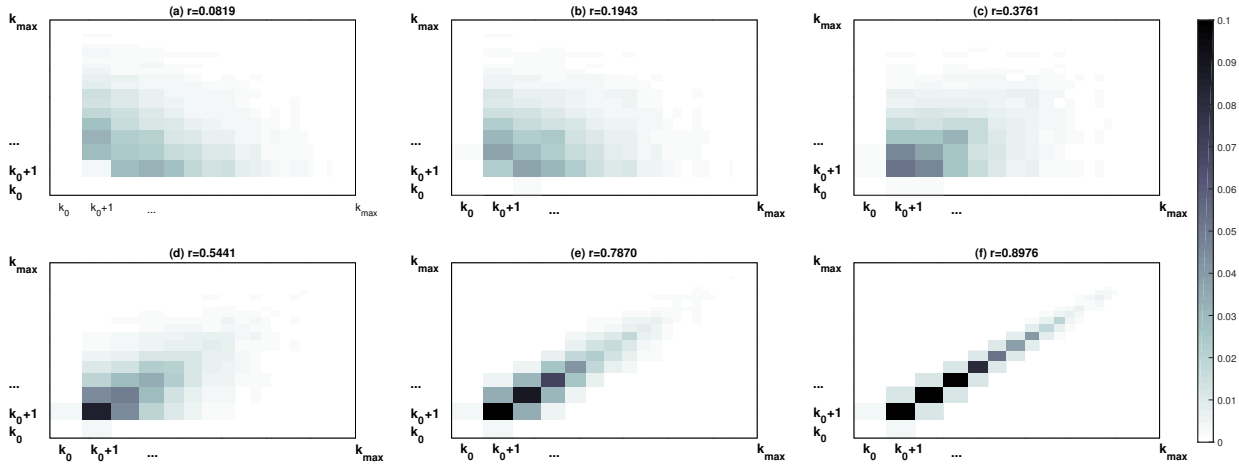


Figure 10: Assortative rewiring: adjacency matrix \mathbf{A} for networks increasing assortativity following Xalvi-Brunet and Sokolov algorithm. $N = 3000$, $\gamma = 2.75$, $\langle k \rangle \approx 4$, $k_0 = 1$. Entries in \mathbf{A} are ordered to increasing node degree k . The colour bar indicates the density of nodes in each cell. Nodes with similar degrees are connected in highly assortative networks.

Assortative rewiring also affects the maximum coreness k_s . With assortative rewiring, while low degree nodes are unaffected, hubs are connected to other hubs and thus become less dependent on the low-degree nodes. The connection between hubs form a more cohesive sub-network at higher k -core [29]. Disassortative rewiring, on the other hand, makes hubs more dependent on low-degree nodes so that the network should have fewer shells. We illustrate this dependency between assortativity (r) and maximum coreness (k_s) in Figure 12.

Appendix B: Epidemic parameter and cumulative incidence

To further assess the risk of measles, we compute the cumulative incidence (CI) during the first outbreak. Cumulative incidence quantifies the proportion of population at risk, defined as the ratio between the number of new cases divided by the total population at risk over a specific period of time. Disease prevalence (I), on the other hand, is measured at one point in time [53]. These two measures are closely related and the cumulative incidence during the first outbreak T is determined as:

$$CI(T) = \sum_{t=1}^T \sum_{j=1}^M \sum_{k=1}^M \beta_j \phi_{ij} \frac{\phi_{kj} I_k}{\epsilon_j^p} S_i \quad (10)$$

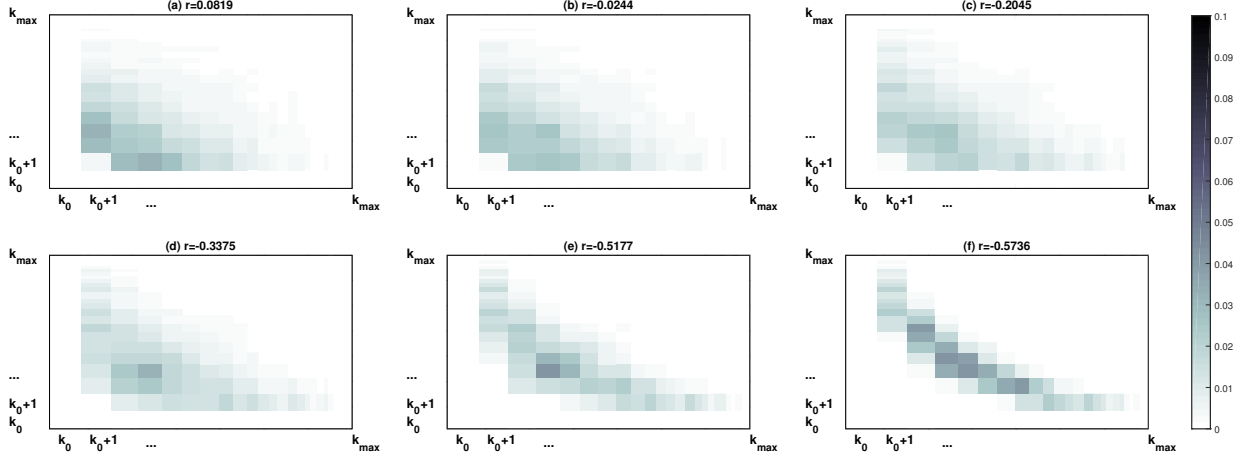


Figure 11: Disassortative rewiring: adjacency matrix \mathbf{A} of networks with decreasing assortativity following Xalvi-Brunet and Sokolov algorithm. $N = 3000, \gamma = 2.75, \langle k \rangle \approx 4, k_0 = 1$. Entries in \mathbf{A} are ordered to increasing node degree k . The color bar indicates the density of nodes in each cell. Nodes with rather different degrees are connected in highly disassortative networks.

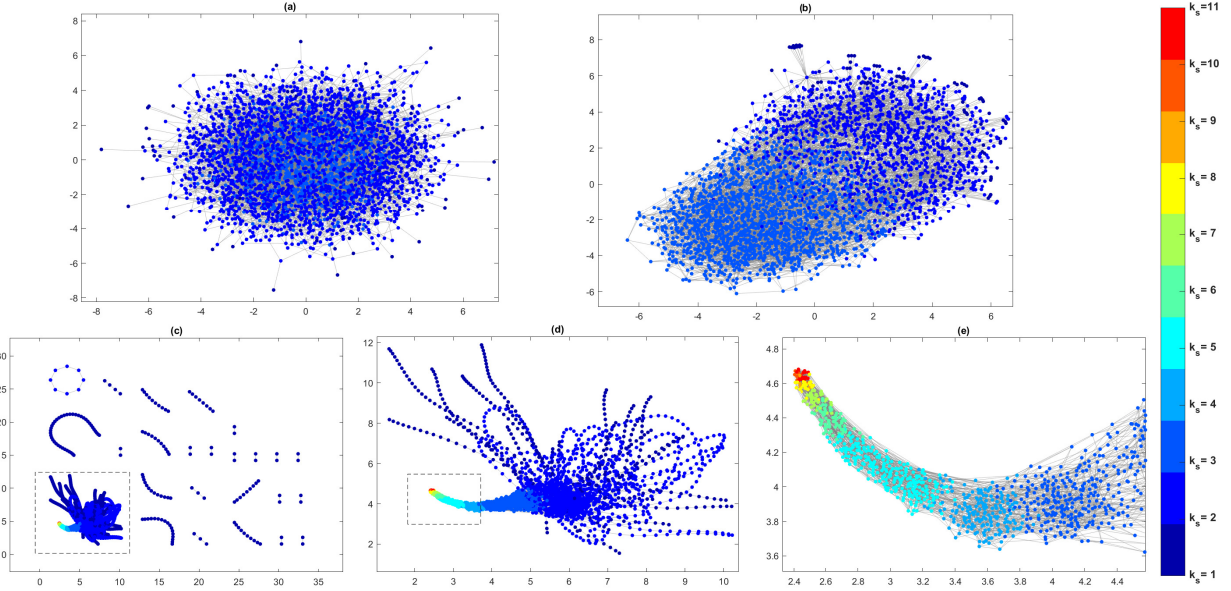


Figure 12: Maximum k_s increases with assortative rewiring. (a) original network $r = 0.0819$, (b) highly disassortative network $r = -0.5736$, (c)-(e) assortative rewiring $r = 0.8976$. Other network properties: $N = 3000, \gamma = 2.75, \langle k \rangle \approx 4, k_0 = 1$.

Where T is measured from initial conditions $t = 0, I_0 = 0.001$ and to the point where the prevalence is below the threshold value $I < \hat{I}$ where $\hat{I} = 0.0002$.

Unless stated otherwise, the behavioural and epidemiological parameters used in simulations are summarised in Table 2.

References

- [1] S. Wiedersehn. Anti-vaxxer movement fuelling global resurgence of measles, say WHO. <https://www.sbs.com.au/news/anti-vaxxer-movement-fuelling-global-resurgence-of-measles-say-who>, 2019. online; last accessed 14 Nov. 2019.
- [2] Department of Helath, New South Wales Government, Australia. 2019-infectious disease alerts, 2019.

parameter	Interpretation	Baseline value	References
β	Transmission rate (day^{-1})	1.5	
$1/\gamma$	Average length of recovery period (days)	10	[7]
R_0	Basic reproduction number	15	[7]
μ	Mean birth and death rate	0.000055	
κ	Imitation rate	0.001	[8]
ω	Responsiveness to changes in disease prevalence	3500	[8]
ϕ_{ij}	Fraction of residents from node i travelling to j	[0,1]	Network connectivity

Table 2: Epidemiological and behavioural parameters. Refer to figure captions for initial conditions for each simulation case.

- [3] P. van den Driessche and J. Watmough. Reproduction numbers and sub-threshold endemic equilibria for compartmental models of disease transmission. *Mathematical Biosciences*, 180:29–48, 2002.
- [4] N. Harding, R. Nigmatullin, and M. Prokopenko. Thermodynamic efficiency of contagions: a statistical mechanical analysis of the sis epidemic model. *Interface Focus*, 8:20180036, 2018.
- [5] E.Y. Erten, J.T. Lizier, M. Piraveenan, and M. Prokopenko. Criticality and information dynamics in epidemiological models. *Entropy*, 19:194, 2017.
- [6] M. Kretzschmar. *International Encyclopedia of Public Health*. Academic Press, 2008.
- [7] F.M. Guerra, S. Bolotin, G. Lim, J. Heffernan, S.L. Deeks, Y. Li, and N. Crowcroft. The basic reproduction number (R_0) of measles: a systematic review. *Lancet Infectious Disease*, 17(12):e420–e428, 2017.
- [8] C. T. Bauch. Imitation dynamics predict vaccinating behaviour. *Proceedings of the Royal Society B*, 272:1669–1675, 2005.
- [9] C. T. Bauch and S. Bhattacharyya. Evolutionary game theory and social learning can determine how vaccine scares unfold. *PLOS Computational Biology*, 8(4), 2012.
- [10] R. Pastor-Satorras and A. Vespignani. Immunization of complex networks. *Physical Review E*, 65:036104, 2002.
- [11] P. Poletti, M. Ajelli, and S. Merler. Risk perception and effectiveness of uncoordinated behavioral responses in an emerging epidemic. *Mathematical Biosciences*, 238:80–89, 2012.
- [12] Z. Wang, Y. Moreno, S. Boccaletti, and M. Perc. Vaccination and epidemics in networked populations — An introduction. *Chaos, solitons & fractals*, 103:177–183, 2017.
- [13] O.M. Cliff, V. Sintchenko, T. C. Sorrell, K. Vadlamudi, N. Mclean, and M. Prokopenko. Network properties of Salmonella epidemics. *Scientific reports*, 9:6159, 2019.
- [14] K. M. Fair, C. Zachreson, and M. Prokopenko. Creating a surrogate commuter network from Australian Bureau of Statistics census data. *Scientific data*, 6:150, 2019.
- [15] O. M. Cliff, M. Harding, M. Piraveen, Y. Erten, M. Gambhir, and M. Prokopenko. Investigating spatiotemporal dynamics and synchrony of influenza epidemics in Australia: an agent-based modelling approach. *Simulation modelling practice and theory*, 87:412–431, 2018.
- [16] C. Zachreson, K.M. Fair, O. M. Cliff, M. Harding, M. Piraveenan, and M. Prokopenko. Urbanization affects peak timing, prevalence, and bimodality of influenza pandemics in Australia: results of a census-calibrated model. *Science advances*, 4:eaau5294, 2018.
- [17] A. Perisic and C.T. Bauch. A simulation analysis to characterize the dynamics of vaccinating behaviour on contact networks. *BMC Infectious Diseases*, 9:77, 2009.
- [18] F. Fu, D.I. Rosenbloom, L. Wang, and M.A. Nowak. Imitation dynamics of vaccination behaviour on social networks. *Proceedings of the Royal Society B*, 278:42–49, 2010.
- [19] Y. Zhang. The impact of other-regarding tendencies on the spatial vaccination network. *Chaos, Solitons & Fractals*, 2013:209–215, 2013.
- [20] X.T. Liu, Z.X. Wu, and L. Zhang. Impact of committed individuals on vaccination behaviour. *Physics Review E*, 86, 2012.
- [21] H. Zhang, F. Fu, W. Zhang, and B. Wang. Rational behaviour is a ‘double-edged sword’ when considering voluntary vaccination. *Physics A*, 391:4807–4815, 2012.

- [22] Q. Wang, C. Du, Y. Geng, and S. Lei. Historical payoff can not overcome the vaccination dilemma on Barabási–Albert scale-free networks. *Chaos, solitons & fractals*, 130:109453, 2020.
- [23] J. Huang, J. Wang, and C. Xia. Role of vaccine efficacy in the vaccination behavior under myopic update rule on complex networks. *Chaos, solitons & fractals*, 130:109425, 2020.
- [24] K. Y. Leung, F. Ball, D. Sirl, and T. Britoon. Individual preventive social distancing during an epidemic may have negative population-level outcomes. *Journal of Royal Society: Interface*, 15(20180296):20180296, 2018.
- [25] L.M. Stolerman, D. Coombs, and S. Boatto. SIR-network model and its application to dengue fever. *Journal of applied mathematics*, 75(6):2581–2609, 2015.
- [26] J. Arino and P. van den Driessche. A multi-city epidemic model. *Mathematical Population Studies*, 10:175–193, 2003.
- [27] S. L. Chang, M. Piraveenan, and M. Prokopenko. The effects of imitation dynamics on vaccination behaviours in sir-network model. *International Journal of Environmental Research and Public Health*, 16:2477, 2019.
- [28] R. Pastor-Satorras, C. Castellano, P.V. Mieghem, and A. Vespignani. Epidemic processes in complex networks. *Reviews of Modern Physics*, 87(287):926–973, 2015.
- [29] M.E.J. Newman. Assortative mixing in networks. *Physical Review Letters*, 89:20, 2002.
- [30] Y. Wang, D. Chakrabarti, C. Wang, and C. Faloutsos. Epidemic spreading in real networks: an eigenvalue viewpoint. In *Proceedings of the 22nd international symposium on reliable distributed systems (SRDS'03)*, 2003.
- [31] A. Jamakovic, R. E. Kooij, P. Van Mieghem, and E. R. van Dam. Robustness of networks against viruses: the role of the spectral radius. In *Symposium on Communications and Vehicular Technology*, 2006.
- [32] M. Kitsak, L. K. Gallos, S. Havlin, F. Liljeros, L. Muchnik, H. E. Stanley, and H.A. Makse. Identification of influential spreaders in complex networks. *Nature Physics*, 6:888–893, 2010.
- [33] K. J. Friston. Functional and effective connectivity in neuroimaging: A synthesis. *Human brain mapping*, 2:56–78, 1994.
- [34] M. E. J. Newman. The structure and function of complex networks. *SIAM Review*, 45:167–256, 2003.
- [35] K. Anand and G. Bianconi. Entropy measures for networks: Toward an information theory of complex topologies. *Physical Review E*, 80:045102, 2009.
- [36] J. T. Lizier, S. Pritam, and M. Prokopenko. Information dynamics in small-world Boolean networks. *Artificial Life*, 17:293–314, 2011.
- [37] X.R. Wang, J. T. Lizier, and M. Prokopenko. Fisher information at the edge of chaos in random Boolean networks. *Artificial Life*, 17:315–329, 2011.
- [38] M. Piraveenan, M. Prokopenko, and A. Y. Zomaya. Local assortativeness in scale-free networks. *Europhysics Letters*, 84:28002, 2008.
- [39] R. E. Solè and S. Valverde. *Complex Networks, Lecture Notes in Physics*, chapter Information theory of complex networks: on evolution and architectural constraints. Springer, 2004.
- [40] M. Piraveenan, M. Prokopenko, and Zomaya A.Y. Assortative mixing in directed biological networks. *IEEE/ACM Transactions on computational biology and bioinformatics*, 9, January/February 2012.
- [41] A. Barabási. *Network Science*. Cambridge University Press, Cambridge, UK, 2016.
- [42] R. Xulvi-Brunet and I. M. Sokolov. Reshuffling scale-free networks: from random to assortative. *Physical Review E*, 70:066102, 2004.
- [43] S. B. Seidman. Network structure and minimum degree. *Social Networks*, 5:269–287, 1983.
- [44] A. Mrvar, A. Batagelj, and W. de Nooy. *Exploratory social network analysis with Pajek*. Cambridge University Press, 2005.
- [45] V. Batagelj and M. Zaversnik. An $o(m)$ algorithm for cores decomposition of networks, 2003.
- [46] D. F. Rueda, E. Calle, and J.L. Marzo. Robustness comparison of 15 real telecommunication networks: structural and centrality measurements. *Journal of network and systems management*, 25:269–289, 2017.
- [47] C.E. Shannon. A mathematical theory of communication. *The Bell System Technical Journal*, 27:379–423, 623–656, 1948.
- [48] M. Piraveenan, M. Prokopenko, and Zomaya A.Y. Assortativeness and information in scale-free networks. *The European Physical Journal B*, 67:291–300, 2009.

- [49] P. Van Mieghem, X. Ge, P. Schumm, S. Trajanovski, and H. Wang. Spectral graph analysis of modularity and assortativity. *Physical Review E*, 82:056113, 2010.
- [50] S. Bhattacharyya and C. T. Bauch. “wait and see” vaccinating behaviour during a pandemic: a game theoretic analysis. *Vaccine*, 29:5519–5525, 2011.
- [51] J. Menche, A. Valleriani, and R. Lipowsky. Asymptotic properties of degree-correlated scale-free networks. *Physical Review E*, 81:046103, 2010.
- [52] G. Csardi and T. Nepusz. The igraph software package for complex network research. *InterJournal, Complex Systems*:1695, 2006.
- [53] P. Buttner and R. Muller. *Epidemiology*. Oxford University Press, 2005.